The conformal bratwurst map and polynomial iterative methods

Tino Koch and Jörg Liesen
Fakultät für Mathematik
Universität Bielefeld
33501 Bielefeld
Germany

September 21, 1998

Abstract

Conformal maps from the exterior of the closed unit disk onto the exterior of 'bratwurst' shape sets in the complex plane are constructed. Using these maps, coefficients for the computation of the corresponding Faber polynomials are derived. The zeros of the Faber polynomials are studied numerically. A 'bratwurst' shape set is the result of deforming an ellipse with foci on the real axis, by conformally mapping the real axis onto the unit circle. Such sets are well suited to serve as general purpose sets for inclusion of sets associated with a matrix, for example the spectrum, field of values or a pseudospectrum. Hence, the sets can be applied in the construction and analysis of polynomial iterative methods for the solution of linear systems. The main advantage of the approach is that the conformal maps are derived from elementary transformations, allowing an easy computation of the transfinite diameter, asymptotic convergence factor and Faber polynomials associated with the 'bratwurst' shape sets. Numerical examples are given.

Key words. polynomial iterative methods, linear systems, convergence analysis, hybrid methods, Faber polynomials, conformal mapping, transfinite diameter

AMS Subject Classifications. 65F10, 30C20, 30C30, 30E10

1 Introduction

In recent years, classical methods of approximation theory have been of considerable interest in the theory of polynomial iterative methods (PIMs) for nonsingular systems of linear equations,

$$A\hat{x} = b,\ A \in \mathbf{C}^{N\times N},\ b \in \mathbf{C}^{N}. \tag{1.1}$$

Given an initial guess x_0 for the solution of (1.1), a PIM is an iterative method yielding iterates x_n which satisfy

$$x_n = x_0 + q_n(A)r_0, \tag{1.2}$$

where $r_0 := b - Ax_0$ is the initial residual and the iteration polynomial $q_n(z)$ is of degree at most $n-1$. The nth residual satisfies

$$r_n := b - Ax_n = p_n(A)r_0,\ \ p_n(z) := 1 - zq_n(z) \in \pi_n, \tag{1.3}$$

where π_n denotes the set of polynomials of degree at most n normalized to have value one at the origin. $p_n(z)$ is called the nth residual polynomial of the PIM, and should be chosen so that r_n is small in some norm specific to the method.

Hybrid PIMs, for example the Arnoldi-Chebyshev [5] and Arnoldi-Faber [27] methods, require the actual *construction* of the iteration polynomials and hence of the residual polynomials. The latter are usually chosen to have small maximum norm on some compact set Ω, which contains (an estimate of) a set associated with the matrix A, for example the spectrum $\Lambda(A)$, or sets containing $\Lambda(A)$, such as the field of values or a pseudospectrum of A. The set Ω is typically referred to as inclusion set. Using methods of approximation theory, polynomials that are asymptotically optimal on inclusion sets can be constructed. These polynomials decrease to zero on the inclusion set with the fastest possible rate, and hence are well suited to serve as residual polynomials of a hybrid PIM. Discussions of different types of inclusion sets used in hybrid PIMs can be found in [18, 22].

On the other hand, parameter free PIMs, for example the Krylov subspace methods MINRES [24], GMRES [25] and QMR [11] (see e.g. [10] for an overview), automatically yield residual polynomials that have certain minimization properties. With methods of approximation theory, upper bounds on the residual norms of these methods can be derived from the minimal maximum norm of the residual polynomials on some compact set associated with the matrix A. Usually, this kind of *analysis* is based on an inclusion set Ω containing $\Lambda(A)$ [25, Proposition 4], the field of values [4] or a pseudospectrum [21, Theorem 4] of A.

The construction and analysis of PIMs can be treated in a unified framework using conformal maps. Let Ψ denote the exterior mapping function of the inclusion set Ω, i.e. the conformal map from the exterior of the closed unit disk onto the exterior of Ω. Then asymptotically optimal normalized polynomials associated with Ω, for example normalized Faber polynomials, can be derived using Ψ. Furthermore, the maximal rate of convergence to zero on Ω of any sequence of polynomials can be computed from the inverse of Ψ evaluated at the point zero.

Since the residual polynomials are normalized to have value one at the point zero, it generally has to be assumed that $0 \notin \Omega$. This presents a major difficulty. Polynomial approximation on a disconnected set such is not well understood and thus one has to work with Ω being connected and compact. But if the origin is inside the convex hull of $\Lambda(A)$, canonical choices for inclusion sets, such as sets bounded by circles or ellipses, include the origin as well. Some authors have to make strong assumptions on the applicability of their methods or convergence bounds. For example, the hybrid Arnoldi-Faber method by Starke and Varga cannot be applied if $\Lambda(A)$ contains real numbers λ_1 and λ_2 with $\lambda_1 < 0 < \lambda_2$ [27, p. 217], and the convergence analysis of Eiermann [4] is not applicable if the origin is in the field of values of A.

A standard approach to the construction or analysis of PIMs is first to find a feasible inclusion set Ω and then to construct the corresponding exterior mapping function Ψ. For sets bounded by ellipses, Ψ is simply the Joukowsky map and the situation is well understood. Asymptotically optimal polynomials as well as asymptotic convergence factors are known [7, 8]. However, as indicated above, such sets are often not feasible and thus the geometry of Ω gets more complicated. Often the boundary of Ω is not chosen to be analytic and in the computation of Ψ, the Schwarz-Christoffel mapping formula is employed. Particular examples of the use of this formula are the hybrid Arnoldi-Faber method [27] as well as the development by Coleman and Myers [1], who compute a conformal map and Faber polynomials for annular sectors. A disadvantage of the Schwarz-Christoffel approach is that the resulting formulas include quantities which are determined implicitly through integral equations. These can only be solved numerically, which is expensive and sometimes susceptible to round-off errors. We refer to [15, Section 16.10] for principal numerical difficulties with Schwarz-Christoffel integrals and to [20, p. 12] for particular difficulties encountered for annular sectors. Moreover, formulas involving implicitly defined quantities often admit only little intuition about the important parameters of the problem.

In this paper, we derive conformal maps from the exterior of the closed unit disk onto the exterior of 'bratwurst' shape sets in the complex plane. A 'bratwurst' shape set is the result of deforming an ellipse with foci on the real axis, by conformally mapping the real axis onto the unit circle, so its boundary is analytic. In its use, such a set is similar to an annular sector and hence is well suited to serve as general purpose inclusion set for sets associated with the matrix A. Our main idea is the following: Using elementary Möbius transformations and the Joukowsky map, we derive conformal maps which we fully control analytically, while the maps can be used as exterior mapping functions of general purpose inclusion regions. As a result, we can easily compute the transfinite diameter (or capacity) as well as the asymptotic convergence factor associated with each 'bratwurst' shape set, while these sets are of broad applicability in the context of PIMs. Because of the simplicity of our approach, we can furthermore derive simple analytic expressions for coefficients to compute the corresponding Faber polynomials. We also study the zeros of these polynomials numerically.

The paper is organized as follows. In Section 2 we collect well known results about the use of conformal maps in the context of PIMs. Section 3 includes the derivation of the conformal maps and definition of the 'bratwurst' shape sets. We give formulas for the corresponding transfinite diameters and asymptotic convergence factors and show that each 'bratwurst' shape set is of bounded boundary rotation. Section 4 deals with the computation of Faber polynomials for the 'bratwurst' shape sets, and Section 5 contains numerical examples.

We denote by $\hat{\mathbf{C}} := \mathbf{C} \cup \{\infty\}$ the extended complex plane and by $\mathbf{E} := \{z : |z| \leq 1\}$ the closed unit disk. If $\mathbf{S}$ is a set in $\hat{\mathbf{C}}$, we denote its complement in $\hat{\mathbf{C}}$ by $\mathbf{S}^C := \hat{\mathbf{C}} \setminus \mathbf{S}$, its boundary by $\partial\mathbf{S}$ and its interior by $int(\mathbf{S})$. If $\mathbf{S}$ is compact, $\|\cdot\|_{\mathbf{S}}$ denotes the maximum norm for functions defined on $\mathbf{S}$.

2 Definitions and preliminaries

We shortly recall the use of conformal maps in our context of approximation theory and state a well known recurrence for computing Faber polynomials. For more details about these classic topics, we refer to [29, Chapters 3-5], [26, Chapters 1-2] and the overview paper [2].

Definition 2.1 *We define the set $\mathcal{E}$ as the collection of all conformal maps $\Psi : \mathbf{E}^C \to \hat{\mathbf{C}}$, which have the following properties:*

(a) $\Psi(\infty) = \infty$.

(b) $\Psi'(\infty) > 0$.

(c) $\Psi(\mathbf{E}^C)$ *is simply connected in* $\hat{\mathbf{C}}$.

(d) $0 \in \Psi(\mathbf{E}^C)$.

Suppose that $\Omega \subset \mathbf{C}$ is compact and that $0 \notin \Omega$ and Ω^C is simply connected in $\hat{\mathbf{C}}$. Then the Riemann mapping theorem guarantees the existence of a unique conformal map

$$\Psi : \mathbf{E}^C \to \Omega^C, \quad \Psi \in \mathcal{E}. \tag{2.1}$$

We call Ψ the exterior mapping function of Ω. The positive real number

$$\Psi'(\infty) =: t > 0 \tag{2.2}$$

is called the transfinite diameter (or capacity) of Ω.

If Ω contains a set associated with a matrix A, the following concepts are used in the analysis and construction of PIMs applied to a linear system with the matrix A (see e.g. [4, 6, 7, 8, 9, 30]).

Definition 2.2 *Suppose that $\Omega \subset \mathbf{C}$ is compact. Then the asymptotic convergence factor for polynomials from π_n associated with Ω is defined by*

$$R(\Omega) := \lim_{n\to\infty} (\inf_{p_n \in \pi_n} \|p_n\|_\Omega)^{1/n}. \tag{2.3}$$

Furthermore, a sequence of polynomials $p_n \in \pi_n$ is called asymptotically optimal for Ω if the $p_n(z)$ satisfy

$$\lim_{n\to\infty} (\|p_n\|_\Omega)^{1/n} = R(\Omega). \tag{2.4}$$

It is easy to see that for $R(\Omega) < 1$, the assumption

$$0 \notin \Omega \tag{2.5}$$

is necessary. On the other hand, it is well known that if $0 \notin \Omega$, then for each $n \geq 0$ the infimum in (2.3) is uniquely attained (see e.g. [26, Chapter 5]). If additionally Ω^C is simply connected in $\hat{\mathbf{C}}$, then $0 < R(\Omega) < 1$ (see e.g. [29, Section 4.7]).

The analysis and construction of PIMs can be treated in a unified way using the exterior mapping function of Ω. First, the asymptotic convergence factor can be computed using the inverse Ψ^{-1},

$$R(\Omega) = \frac{1}{|\Psi^{-1}(0)|} \tag{2.6}$$

(see e.g. [29, Section 4.7]). Next, Ψ and its inverse can be expanded as

$$\Psi(z) = t\left(z + \alpha_0 + \frac{\alpha_1}{z} + \frac{\alpha_2}{z^2} + \ldots\right). \tag{2.7}$$

and

$$\Psi^{-1}(z) = \frac{z}{t} + \beta_0 + \frac{\beta_1}{z} + \frac{\beta_2}{z^2} + \ldots. \tag{2.8}$$

The part in the expansion of $[\Psi^{-1}(z)]^n$, $n \geq 0$, which contains the nonnegative powers of z is called the nth Faber polynomial $F_n(z)$ for Ω. Obviously, $F_0(z) \equiv 1$ and $F_n(z)$ is of exact degree n with leading term $(z/t)^n$.

With the coefficients α_k in the expansion of Ψ, a well known recurrence for the Faber polynomials is given by

$$F_1(z) = z/t - \alpha_0, \tag{2.9}$$

$$F_{n+1}(z) = F_1(z)F_n(z) - n\alpha_n - \sum_{k=1}^{n} \alpha_k F_{n-k}(z), \quad n \geq 1 \tag{2.10}$$

(see e.g. [2, Section 2]).

Numerical and theoretical properties of normalized Faber polynomials,

$$\tilde{F}_n(z) := \frac{F_n(z)}{F_n(0)} \in \pi_n, \quad n \geq 0, \tag{2.11}$$

have been extensively studied (see e.g. [3, 27, 20]). These are asymptotically optimal if Ω is convex or of bounded boundary rotation (cf. [27, Theorems 3.1 and 3.3] [1]), and hence in these cases are well suited for the construction of a hybrid PIM. Details on implementations of such methods, particularly the efficient computation of the iterates, can be found in [3, 27].

[1]We remark that the definition of the boundary rotation of a compact set Ω used by Starke and Varga (see [27, Formula (3.6)]) is not the same as the classical definition as given in [23, p.

3 Inclusion sets generated by the conformal bratwurst map

To explain our motivation for deriving exterior mapping functions of 'bratwurst' shape sets, we briefly review the general purpose inclusion sets that have been used in the literature about PIMs. These can be roughly divided into two classes.

The first class consists of convex sets with analytic boundary and very simple geometry, for example disks [25, Theorem 5] and sets bounded by ellipses [7, 8]. The geometry of these sets allows an easy computation of asymptotic convergence factors and of asymptotically optimal polynomials. But because of the general constraint that the origin has to be outside the inclusion set, the convexity leads to limited applicability of the results.

The second class consists of non-convex sets with a more complicated geometry and non-analytic boundary, for example annular sectors [1, 20] and (non-convex) sets bounded by polygons [18, 27]. But while the non-convexity of these sets leads to broader applicability, the non-analytic boundary makes the computation of the exterior mapping function difficult. We have indicated these difficulties in the introduction.

With our approach we want to generate inclusion sets that combine the best of both worlds, general applicability and inexpensive computation of associated quantities. In particular, our sets should be non-convex and have an analytic boundary.

Theorem 3.1 *Let $\lambda_m \in \partial \mathbf{E}$ and $\phi \in (0, 2\pi)$ be given. Define*

$$\epsilon_{max} := \tan\frac{\phi}{4}\left(1+\tan\frac{\phi}{8}\right), \quad \text{and} \quad P := \tan\frac{\phi}{4} + \cos^{-1}\frac{\phi}{4}. \tag{3.1}$$

Then for each $\epsilon \in [0, \epsilon_{max})$, the function

$$\Psi_\epsilon(z) = \frac{(z-\lambda_m N_\epsilon)(z-\lambda_m M_\epsilon)}{(N_\epsilon - M_\epsilon)z + \lambda_m(N_\epsilon M_\epsilon - 1)}, \tag{3.2}$$

where

$$N_\epsilon = \frac{1}{2}\left(\frac{P}{1+\epsilon} + \frac{1+\epsilon}{P}\right), \quad \text{and} \quad M_\epsilon = \frac{(1+\epsilon)^2 - 1}{2\tan\frac{\phi}{4}(1+\epsilon)}, \tag{3.3}$$

is an element of $\mathcal{E}$. Furthermore, if we define $\Omega_\epsilon := \Psi_\epsilon(\mathbf{E}^C)^C$, then $\lambda_m \notin \Omega_\epsilon$ and $\left\{\lambda_m e^{i\beta} \;:\; \phi/2 \le \beta \le 2\pi - \phi/2\right\} \subseteq \Omega_\epsilon$.

Proof. Our constructive proof makes extended use of Möbius transformations

$$\psi(z) = \frac{az+b}{cz+d}, \quad ad - bc \neq 0, \quad a, b, c, d \in \mathbf{C},$$

which build the group of conformal automorphisms of $\hat{\mathbf{C}}$. We will exhibit the function Ψ_ϵ with the stated properties as the composition of three relatively simple conformal maps,

$$\Psi_\epsilon = \psi_2 \circ J \circ \psi_1.$$

We first give an overview of the construction. Suppose that $\epsilon > 0$. Then ψ_1 is a certain Möbius transformation that maps $\mathbf{E}^C$ on $|z| > 1+\epsilon$. We next apply the Joukowsky map

$$J(z) = \frac{1}{2}\left(z + z^{-1}\right).$$

5] (also cf. [17, p. 197]). In particular, the definition used in [27] gives only a lower bound on the classical boundary rotation (cf. [12, p. 49]). But by modifying the proofs of [27, Theorems 3.1 and 3.3], it can be easily shown that normalized Faber polynomials are asymptotically optimal if Ω is of bounded boundary rotation in the sense of the classical definition as well.

For each $r \geq 1$, J maps the set $|z| > r$ conformally onto the exterior of an ellipse with foci ± 1 and semiaxes $\left(r \pm r^{-1}\right)/2$. Hence, $(J \circ \psi_1)(\mathbf{E}^C)$ is the complement of the ellipse with foci ± 1 and semiaxes $\left((1+\epsilon) \pm (1+\epsilon)^{-1}\right)/2$. Finally, the Möbius transformation ψ_2 maps the real axis on the unit circle such that the image of $(J \circ \psi_1)(\mathbf{E}^C)$ under ψ_2 is Ω_ϵ^C, and Ω_ϵ has the stated property.

In detail, since ψ_2 is conformal it transforms one of the halfplanes

$$\mathbf{H_U} := \{z \,:\, Im(z) > 0\} \;\text{ or }\; \mathbf{H_L} := \{z \,:\, Im(z) < 0\}$$

to $int(\mathbf{E})$. Let $\mathcal{C}(\Omega^1, \Omega^2)$ denote the set of all conformal maps from Ω^1 to Ω^2. If $\tau_1,\, \tau_2 \in \mathcal{C}(\mathbf{H_U}, int(\mathbf{E}))$, then $\tau_2 \circ \tau_1^{-1} \in \mathcal{C}(int(\mathbf{E}), int(\mathbf{E}))$. It is a classical result in complex function theory that each such mapping is of the form

$$f(z) = e^{i\theta}\frac{z+c}{\bar{c}z+1}, \quad |c| < 1, \quad \theta \in \mathbf{R} \tag{3.4}$$

(see e.g. [16, Chapter 15]). Together with the Cayley map $\tau_C(z) = (z-i)/(z+i) \in \mathcal{C}(\mathbf{H_U}, int(\mathbf{E}))$, a direct calculation yields

$$\mathcal{C}(\mathbf{H_U}, int(\mathbf{E})) = \left\{ e^{i\theta}\frac{z-s}{z-\bar{s}} \;:\; \theta \in \mathbf{R},\; s \in \mathbf{H_U} \right\}. \tag{3.5}$$

The function $\psi : \mathbf{H_U} \to \mathbf{H_L}$, $\psi(z) = -z$, shows that

$$\mathcal{C}(\mathbf{H_L}, int(\mathbf{E})) = \left\{ e^{i\theta}\frac{z+s}{z+\bar{s}} \;:\; \theta \in \mathbf{R},\; s \in \mathbf{H_U} \right\}. \tag{3.6}$$

For our purpose we fix $\psi_2 \in \mathcal{C}(\mathbf{H_L}, int(\mathbf{E}))$. To guarantee that $\Omega_\epsilon := \Psi_\epsilon(\mathbf{E}^C)^C$ satisfies $\lambda_m \notin \Omega_\epsilon$ and $\left\{\lambda_m e^{i\beta} \;:\; \frac{\phi}{2} \leq \beta \leq 2\pi - \frac{\phi}{2}\right\} \subseteq \Omega_\epsilon$, we set

$$\psi_2(-1) = \lambda_m e^{-i\phi/2}, \quad \psi_2(1) = \lambda_m e^{i\phi/2}, \quad \psi_2(\infty) = \lambda_m. \tag{3.7}$$

These properties yield

$$\psi_2(z) = \lambda_m \frac{z + i\tan\frac{\phi}{4}}{z - i\tan\frac{\phi}{4}}. \tag{3.8}$$

Observe that $\psi_2\left(i\tan\frac{\phi}{4}\right) = \infty$. To have $\Psi_\epsilon \in \mathcal{E}$, we have to satisfy $(a) - (d)$ of Definition 2.1. To satisfy (a) and (d), we require

$$\Psi_\epsilon(\infty) = \infty \;\text{ and }\; 0 \in \Psi_\epsilon(\mathbf{E}^C). \tag{3.9}$$

We define

$$P_\infty := J^{-1}\left(i\tan\frac{\phi}{4}\right)$$

by taking the branch of the inverse Joukowsky map, $J^{-1}(z) = z + (z^2-1)^{1/2}$, that gives the greatest possible modulus $|P_\infty|$, and compute

$$P_\infty = i\left(\tan\frac{\phi}{4} + \cos^{-1}\frac{\phi}{4}\right). \tag{3.10}$$

The preimages of ∞ and 0 under ψ_2 are complex conjugates and so they are under $\psi_2 \circ J$, i.e.,

$$(\psi_2 \circ J)(P_\infty) = \infty \;\text{ and }\; (\psi_2 \circ J)\left(\overline{P_\infty}\right) = 0. \tag{3.11}$$

To actually satisfy both conditions in (3.9), which now are closely related by P_∞ and $\overline{P_\infty}$, we need that $P_\infty \in \psi_1(\mathbf{E}^C) = \{z \,:\, |z| > 1+\epsilon\}$. But this holds if ϵ satisfies

$$0 \leq \epsilon < |P_\infty| - 1 = \tan\frac{\phi}{4}\left(1 + \tan\frac{\phi}{8}\right) =: \epsilon_{max}. \tag{3.12}$$

The still unknown function ψ_1 can be written as

$$\psi_1(z) = (1+\epsilon)\rho(z),$$

where ρ is a conformal self-mapping of $\mathbf{E}$ and hence is of the form (3.4). Note that ρ has to satisfy $\rho(\infty) = P_\infty/(1+\epsilon)$, which implies $c = e^{-i\theta}(1+\epsilon)/(\overline{P_\infty})$. We choose $e^{i\theta} = -i\lambda_m^{-1}$. As we will see, this choice leads to a conformal map Ψ_ϵ that satisfies the condition (b) of Definition 2.1, i.e. $\Psi_\epsilon'(\infty) > 0$. First, we give the resulting analytic terms for

$$\psi_1(z) = (1+\epsilon)\frac{iP_\infty z + \lambda_m(1+\epsilon)}{i(1+\epsilon)z + \lambda_m \overline{P_\infty}} \text{ and } \psi_1^{-1}(z) = \frac{i\lambda_m}{1+\epsilon}\frac{\overline{P_\infty} z - (1+\epsilon)^2}{z + \overline{P_\infty}}. \tag{3.13}$$

So far, we have constructed

$$\Psi_\epsilon(z) = (\psi_2 \circ J \circ \psi_1)(z) = \lambda_m \frac{\psi_1^2(z) + 2i\tan\frac{\phi}{4}\psi_1(z) + 1}{\psi_1^2(z) - 2i\tan\frac{\phi}{4}\psi_1(z) + 1}. \tag{3.14}$$

According to (3.14), Ψ_ϵ is a rational function of z, the denominator and numerator of which are polynomials of degree at most 2. To simplify (3.14), we ask for the preimages of 0 and ∞ under Ψ_ϵ or, in other words, for the roots of the numerator and denominator. From (3.11) together with the fact that $J(z) = J(z^{-1})$ for all $z \in \hat{\mathbf{C}}$ follows that

$$\begin{aligned} 0 &= \Psi_\epsilon\left(\psi_1^{-1}(\overline{P_\infty})\right) = \Psi_\epsilon\left(\psi_1^{-1}\left(\frac{1}{\overline{P_\infty}}\right)\right) \quad \text{and} \\ \infty &= \Psi_\epsilon\left(\psi_1^{-1}(P_\infty)\right) = \Psi_\epsilon\left(\psi_1^{-1}\left(\frac{1}{P_\infty}\right)\right) = \Psi_\epsilon(\infty). \end{aligned} \tag{3.15}$$

Hence, for the zeros of Ψ_ϵ we have

$$N_\epsilon := \frac{1}{\lambda_m}\,\psi_1^{-1}(\overline{P_\infty}) \text{ and } M_\epsilon := \frac{1}{\lambda_m}\,\psi_1^{-1}(1/\overline{P_\infty}). \tag{3.16}$$

An easy calculation shows that N_ϵ and M_ϵ are of the form stated in (3.3). Clearly, only one of these zeros lies in $\mathbf{E}^C$. In fact, for all $\epsilon \in [0, \epsilon_{max})$ we have

$$M_\epsilon < 1 < N_\epsilon. \tag{3.17}$$

Similarly, since ∞ is a fixpoint of Ψ_ϵ, the second preimage of ∞ lies in $int(\mathbf{E})$. It can be expressed as a surprisingly simple rational function of the zeros,

$$\psi_1^{-1}\left(\frac{1}{P_\infty}\right) = \frac{\lambda_m P}{1+\epsilon}\frac{(1+\epsilon)^2+1}{P^2+1} = \lambda_m \frac{1 - N_\epsilon M_\epsilon}{N_\epsilon - M_\epsilon}, \tag{3.18}$$

where $P := |P_\infty|$. Thus, the function Ψ_ϵ we have constructed is of the form (3.2), namely

$$\Psi_\epsilon(z) = \frac{(z - \lambda_m N_\epsilon)(z - \lambda_m M_\epsilon)}{(N_\epsilon - M_\epsilon)z + \lambda_m(N_\epsilon M_\epsilon - 1)}.$$

To complete the proof we easily check that

$$\Psi_\epsilon'(\infty) = \lim_{z\to\infty}\frac{\Psi_\epsilon(z)}{z} = \frac{1}{N_\epsilon - M_\epsilon} > 0$$

(cf.(3.17)). Furthermore, referring to (c) of the definition of $\mathcal{E}$, we remark that $\Psi_\epsilon(\mathbf{E}^C)$ obviously is simply connected in $\hat{\mathbf{C}}$. $\square$

Example 3.2 (Circular arc) Suppose that some $\lambda_m \in \partial\mathbf{E}$ and $\phi \in (0, 2\pi)$ are given. If we choose $\epsilon = 0$, then $N_\epsilon = \cos^{-1}\frac{\phi}{4}$ and $M_\epsilon = 0$. Thus, Ψ_ϵ in (3.2) reduces to

$$\Psi_\epsilon(z) = \frac{z(z\cos\frac{\phi}{4} - \lambda_m)}{z - \lambda_m \cos\frac{\phi}{4}}. \tag{3.19}$$

This function maps $\mathbf{E}^C$ onto the exterior of the circular arc $\{\lambda_m e^{i\beta} \;:\; \phi/2 \leq \beta \leq 2\pi - \phi/2\}$. We point out that, allowing for the difference in notation, Ψ_ϵ in (3.19) is the same as the mapping function derived by Coleman and Myers for the same purpose (cf. [1, Formula (2.19)]). In light of the uniqueness guaranteed by the Riemann mapping theorem, this is certainly not a surprise.

We now use Theorem 3.1 to define a class of sets which are well suited to serve as general purpose inclusion sets.

Definition 3.3 *Suppose that some $\lambda_m \in \partial\mathbf{E}$ and $\phi \in (0, 2\pi)$ are given and the corresponding ϵ_{max} is given as in (3.1). Using Ψ_ϵ as in (3.2), we define the class of sets $\mathbf{B}(\lambda_m, \phi)$ by*

$$\mathbf{B}(\lambda_m, \phi) := \left\{ \Omega_\epsilon \;:\; \Omega_\epsilon = \left(\Psi_\epsilon(\mathbf{E}^C)\right)^C, \; \epsilon \in [0, \epsilon_{max}) \right\}. \tag{3.20}$$

The following important properties of each $\Omega_\epsilon \in \mathbf{B}(\lambda_m, \phi)$ follow directly from properties of the generating conformal map Ψ_ϵ.

Corollary 3.4 *For each $\Omega_\epsilon \in \mathbf{B}(\lambda_m, \phi)$ the following hold:*

(a) $0 \notin \Omega_\epsilon$ and $\lambda_m \notin \Omega_\epsilon$.

(b) The transfinite diameter of Ω_ϵ is $t(\Omega_\epsilon) = 1/(N_\epsilon - M_\epsilon)$.

(c) $R(\Omega_\epsilon) = 1/N_\epsilon$.

(d) Ω_ϵ is simply connected.

As one could expect, $t(\Omega_\epsilon)$ and $R(\Omega_\epsilon)$ are independent of λ_m, i.e. invariant under rotation. The simplicity of our approach demonstrates the dependence of $t(\Omega_\epsilon)$ and $R(\Omega_\epsilon)$ on the other parameters, ϵ and ϕ. We will briefly analyze this dependence for $R(\Omega_\epsilon)$. First note that the modulus of P in (3.3) is strictly increasing with increasing angle ϕ. Hence, for each fixed ϵ, $R(\Omega_\epsilon)$ strictly decreases with increasing ϕ. The same is true for fixed ϕ and decreasing ϵ. In this case, as ϵ ranges from ϵ_{max} to zero, $R(\Omega_\epsilon)$ ranges from one to $\cos\frac{\phi}{4}$.

Intuitively, ϵ controls the 'thickness' of $\Omega_\epsilon \in \mathbf{B}(\lambda_m, \phi)$. The dependence on ϵ of the shape of Ω_ϵ is not completely obvious. Sometimes, several choices of ϵ have to be tested until Ω_ϵ contains the required region. However, the check on ϵ is computationally cheap. Because $\partial\Omega_\epsilon = \Psi_\epsilon(\partial\mathbf{E})$, one simply has to evaluate Ψ_ϵ at a few points of $\partial\mathbf{E}$.

Lemma 3.5 *Each $\Omega_\epsilon \in \mathbf{B}(\lambda_m, \phi)$ is of bounded boundary rotation.*

Proof. We first recall the classical definition of the total rotation of an analytic Jordan curve $\Gamma = z(t)$ [23] (also cf. [17]). Let $\theta(t)$ denote the angle between the positive real axis and the tangent of Γ at the point $z(t)$. Then the total rotation of Γ is defined as the total variation of θ, i.e. the Stieltjes integral

$$\int_\Gamma |d\theta|.$$

Accordingly, the boundary rotation of a Jordan domain Ω with analytic boundary $\partial\Omega$ is defined as

$$V(\Omega) := \int_{\partial\Omega} |d\theta|. \tag{3.21}$$

Now suppose that some set $\Omega_\epsilon \in \mathbf{B}(\lambda_m, \phi)$ is given with $\epsilon > 0$. From the construction it is easy to see that Ψ_ϵ can be extended holomorphically into a full neighborhood of $\partial\mathbf{E}$. Hence $\Psi_\epsilon(\partial\mathbf{E}) = \partial\Omega_\epsilon$ is an analytic Jordan curve and the corresponding function $\theta(t)$ is given by

$$\theta(t) = \frac{\pi}{2} + t + \arg \Psi_\epsilon'(e^{it})$$

(cf. e.g. [19, Chapter 8]), where we denote

$$\Psi_\epsilon'(e^{it}) = \left.\frac{d}{dz}\Psi_\epsilon(z)\right|_{z=e^{it}}.$$

Therefore,

$$\begin{aligned} V(\Omega_\epsilon) &= \int_{\partial\Omega_\epsilon} |d\theta| = \int_{t=0}^{2\pi} \left| d\left(\frac{\pi}{2} + t + \arg\Psi_\epsilon'(e^{it})\right)\right| \\ &= \int_0^{2\pi} \left|\frac{d}{dt}\left(\frac{\pi}{2} + t + \arg\Psi_\epsilon'(e^{it})\right)\right| dt \\ &= \int_0^{2\pi} \left|1 + \frac{d}{dt}\arg\Psi_\epsilon'(e^{it})\right| dt \le 2\pi + \int_0^{2\pi} \left|\frac{d}{dt}\arg\Psi_\epsilon'(e^{it})\right| dt. \end{aligned}$$

From elementary considerations it follows, that for $z = e^{it}$,

$$\frac{d}{dt}\arg\Psi_\epsilon'(z) = Re\left(\frac{z\Psi_\epsilon''(z)}{\Psi_\epsilon'(z)}\right).$$

But since Ψ_ϵ is conformal, $\Psi_\epsilon'(z) \neq 0$ on $\partial\mathbf{E}$, so that this defines a continuous function on $\partial\mathbf{E}$. From this we easily conclude that $V(\Omega_\epsilon) < \infty$, i.e. Ω_ϵ is of bounded boundary rotation. To complete the proof, we remark that for $\epsilon = 0$, Ω_ϵ is a degenerated annular sector and hence of bounded boundary rotation. In this case, a formula for $V(\Omega_\epsilon)$ is given in [1, p. 200]. □

In applications it is often interesting to scale the elements of $\mathbf{B}(\lambda_m, \phi)$, i.e. to form sets

$$s\Omega_\epsilon := \{sz \;:\; z \in \Omega_\epsilon\}, \quad s > 0. \tag{3.22}$$

Properties of these scaled sets are easily derived.

Lemma 3.6 *Suppose that $s > 0$ and $\Omega_\epsilon \in \mathbf{B}(\lambda_m, \phi)$. Then $s\Omega_\epsilon$ satisfies properties (a), (c) and (d) of Corollary 3.4, and $t(s\Omega_\epsilon) = s\,t(\Omega_\epsilon)$.*

Proof. If we define $\psi(z) := sz$, then $s\Omega_\epsilon = \big((\psi \circ \Psi_\epsilon)(\mathbf{E}^C)\big)^C$. Now the assertions are immediate consequences of the properties of $\psi \circ \Psi_\epsilon$. □

Lemma 3.6 shows in particular that the asymptotic convergence factor associated with a set $\Omega_\epsilon \in \mathbf{B}(\lambda_m, \phi)$ is invariant under scaling of the set.

4 Faber polynomials for the inclusion sets

Suppose that Ψ_ϵ as in (3.2) is the exterior mapping function of some given set $\Omega_\epsilon \in \mathbf{B}(\lambda_m, \phi)$.

We define

$$S_\epsilon := -\frac{N_\epsilon M_\epsilon - 1}{N_\epsilon - M_\epsilon}, \tag{4.1}$$

then Ψ_ϵ in (3.2) can be expanded as

$$\begin{aligned} \Psi_\epsilon(z) &= \frac{1}{N_\epsilon - M_\epsilon}\Big(z - \lambda_m(N_\epsilon + M_\epsilon - S_\epsilon) + \\ &+ \lambda_m^2(S_\epsilon - N_\epsilon)(S_\epsilon - M_\epsilon)\sum_{n=1}^{\infty}(\lambda_m S_\epsilon)^{n-1} z^{-n}\Big). \end{aligned} \tag{4.2}$$

This shows the following Lemma.

Lemma 4.1 *Suppose that $\lambda_m \in \partial\mathbf{E}$ and $\phi \in (0, 2\pi)$ are given. If $\Omega_\epsilon \in \mathbf{B}(\lambda_m, \phi)$, the coefficients for the computation of the Faber polynomials $F_n(z)$ for $s\Omega_\epsilon$, $s > 0$, as in (2.9) and (2.10), are*

$$t = s/(N_\epsilon - M_\epsilon), \;\; \alpha_0 = -\lambda_m(N_\epsilon + M_\epsilon - S_\epsilon), \tag{4.3}$$

and

$$\alpha_n = (\lambda_m S_\epsilon)^{n-1}\lambda_m^2(S_\epsilon - N_\epsilon)\,(S_\epsilon - M_\epsilon), \;\; n \geq 1. \tag{4.4}$$

We next derive expressions for the coefficients α_n in terms of trigonometric functions.

Lemma 4.2 *In the notation of Lemma 4.1,*

$$\alpha_0 = -\lambda_m \frac{\big((1+\epsilon)^2 - 1\big)\cos\frac{\phi}{2} + \big(1 + (1+\epsilon)^2\big)\sin^3\frac{\phi}{4}}{2(1+\epsilon)\cos\frac{\phi}{4}\sin\frac{\phi}{4}}, \tag{4.5}$$

and for $n \geq 1$,

$$\alpha_n = -\lambda_m^{n+1}\frac{\big(1+(1+\epsilon)^2\big)^{n-1}\cos^{n-1}\frac{\phi}{4}}{\big(2(1+\epsilon)\big)^{n+1}}\left(1 - (1+\epsilon)^2 + (1+(1+\epsilon)^2)\sin\frac{\phi}{4}\right)^2. \tag{4.6}$$

Proof. The proof is technical and consists of resubstitutions and applications of relations between trigonometric functions. We therefore omit the details here. The identities

$$\begin{aligned} N_\epsilon M_\epsilon - 1 &= \frac{(1+\epsilon)^4 - 1 - \big(1+(1+\epsilon)^2\big)^2\sin\frac{\phi}{4}}{4(1+\epsilon)^2\sin\frac{\phi}{4}} \quad \text{and} \\ \frac{1}{N_\epsilon - M_\epsilon} &= \frac{2(1+\epsilon)\sin\frac{\phi}{4}\cos\frac{\phi}{4}}{1 - (1+\epsilon)^2 + (1+(1+\epsilon)^2)\sin\frac{\phi}{4}} \end{aligned} \tag{4.7}$$

can be proven directly. We use them and (4.1) to calculate

$$S_\epsilon = \frac{1 + (1+\epsilon)^2}{2(1+\epsilon)}\cos\frac{\phi}{4}. \tag{4.8}$$

Using (4.8), we can easily show (4.5). To complete the material we state

$$S_\epsilon - N_\epsilon = -\frac{1-(1+\epsilon)^2 + \left(1+(1+\epsilon)^2\right)\sin\frac{\phi}{4}}{2(1+\epsilon)\cos\frac{\phi}{4}} \sin\frac{\phi}{4}, \tag{4.9}$$

$$S_\epsilon - M_\epsilon = \frac{1-(1+\epsilon)^2 + \left(1+(1+\epsilon)^2\right)\sin\frac{\phi}{4}}{2(1+\epsilon)\sin\frac{\phi}{4}} \cos\frac{\phi}{4}. \tag{4.10}$$

An easy direct calculation now leads to (4.6). □

Note that from (4.8) follows that $0 < S_\epsilon < 1$. Hence, $\alpha_n \to 0$, as $n \to \infty$. We conclude that the Faber polynomials for $s\Omega_\epsilon$ can be computed in a numerically cheap and stable way.

Since the elements of $\mathbf{B}(\lambda_m, \phi)$ are of bounded boundary rotation (cf. Lemma 3.5), the corresponding scaled Faber polynomials are asymptotically optimal, which potentially yields a quickly converging method. We will use these polynomials as residual polynomials for the construction of a hybrid PIM in a forthcoming paper.

We now turn to the computation of the zeros of the Faber polynomials for elements of $\mathbf{B}(\lambda_m, \phi)$. If $F_n(z)$, $n \geq 0$, is the nth Faber polynomial of $s\Omega_\epsilon$, we define the scaled Faber polynomial $\check{F}_n(z)$ by

$$\check{F}_n(z) := t^n F_n(z), \quad n \geq 0, \tag{4.11}$$

where $t = s/(N_\epsilon - M_\epsilon)$ is the transfinite diameter of $s\Omega_\epsilon$. Obviously, the zeros of $F_n(z)$ and $\check{F}_n(z)$ are identical. Using (2.9) and (2.10), it is easy to show that the $\check{F}_n(z)$ satisfy

$$\check{F}_1(z) = z - a_0, \tag{4.12}$$

$$\check{F}_{n+1}(z) = \check{F}_1(z)\check{F}_n(z) - na_n - \sum_{k=1}^{n} a_k \check{F}_{n-k}(z), \quad n \geq 1, \tag{4.13}$$

where $a_k := t^{k+1}\alpha_k$, $k \geq 0$. Note that (4.12) and (4.13) have the well known determinant representation

$$\check{F}_n(z) = det(zI_n - H_n), \quad n \geq 1 \tag{4.14}$$

(see e.g. [14, Theorem 3.1]), where

$$H_n = \begin{bmatrix} a_0 & 1 & 0 & \cdots & \cdots & 0 \\ 2a_1 & a_0 & 1 & \ddots & & \vdots \\ 3a_2 & a_1 & a_0 & \ddots & \ddots & \vdots \\ \vdots & \vdots & \vdots & & \ddots & 0 \\ (n-1)a_{n-2} & a_{n-3} & a_{n-4} & \cdots & a_0 & 1 \\ na_{n-1} & a_{n-2} & a_{n-3} & \cdots & a_1 & a_0 \end{bmatrix}. \tag{4.15}$$

Thus, the zeros of $F_n(z)$, $n \geq 1$, are the eigenvalues of the matrix H_n. We use this for numerical computations of the zeros of Faber polynomials in the following section.

5 Numerical examples

All numerical computations in this section were performed using the software MATLAB 5.0 [28].

Example 5.1 We show what typical elements of $\mathbf{B}(\lambda_m, \phi)$ look like and how the transfinite diameter and asymptotic convergence factor change with changing parameter ϵ. Suppose that $\lambda_m = -1$ and $\phi = \pi/2$. Then $\epsilon_{max} \approx 0.4966$. In Figure 1 we plot $\partial\Omega_\epsilon$ for $\Omega_\epsilon \in \mathbf{B}(-1, \pi/2)$ and $\epsilon = 0, 0.05, 0.1$, and 0.15. λ_m and the origin are indicated as '$*$'. The corresponding transfinite diameters and asymptotic convergence factors were computed using Corollary 3.4 and are listed in the following table.

ϵ	0	0.05	0.1	0.15
$t(\Omega_\epsilon)$	0.9239	1.0575	1.2235	1.4360
$R(\Omega_\epsilon)$	0.9239	0.9403	0.9544	0.9633

Example 5.2 We compare elements of $\mathbf{B}(\lambda_m, \phi)$ to annular sectors

$$\mathbf{S}(\lambda_m, \phi, h) := \left\{ r\lambda_m e^{i\beta} \ : \ \phi/2 \leq \beta \leq 2\pi - \phi/2, \ \ h \leq r \leq 1 \right\},$$

which have been proposed in the literature as general purpose inclusion sets. Using Gaussian quadrature to evaluate a formula derived by Coleman and Myers [1] with the Schwarz-Christoffel approach, Modersitzki and Opfer compute transfinite diameters of $\mathbf{S}(1, \phi, 1/2)$ for some values of ϕ. To obtain a high accuracy, the effort of this computation is 'quite high' [20, p.15]. We scaled corresponding elements of $\mathbf{B}(1, \phi)$ by $s = 3/4$, chose a suitable ϵ and computed the transfinite diameter and asymptotic convergence factor using Lemma 3.6. ϵ was chosen so that $\frac{3}{4}\Omega_\epsilon$ contains roughly the same region as the corresponding $\mathbf{S}(1, \phi, 1/2)$. The particular choices were $\epsilon = 0.1$ and $\epsilon = 0.2$ for $\phi = \pi/2$ and $\phi = \pi$, respectively. Plots of the respective boundaries are shown in Figures 2 and 3, numerical results are listed in the table below. The results about $\mathbf{S}(1, \phi, 1/2)$ are taken from [20, Table 7.1].

ϕ, ϵ	$R(\frac{3}{4}\Omega_\epsilon)$	$t(\frac{3}{4}\Omega_\epsilon)$	$t(\mathbf{S}(1, \phi, 1/2))$
$\pi/2$, 0.1	0.9544	0.9176	0.9382
π, 0.2	0.7972	0.7002	0.7587

Example 5.3 We show the inclusion of matrix spectra by elements of $\mathbf{B}(\lambda_m, \phi)$. The spectra were computed using MATALB's `eig` function.

The first example spectrum comes from a matrix of the GRCAR family. Because of the special geometry of their spectra, GRCAR matrices are standard examples in this context (see e.g. [27, Example 6.3] and [22, Example 2]). Our particular choice is the matrix

$$A = \begin{bmatrix} 1 & 1 & \cdots & 1 & & & & \\ -1 & 1 & 1 & \cdots & 1 & & & \\ & \ddots & \ddots & \ddots & & & \ddots & \\ & & -1 & 1 & 1 & & \cdots & 1 \\ & & & \ddots & \ddots & & \ddots & \vdots \\ & & & & \ddots & & \ddots & 1 \\ & & & & & & -1 & 1 \end{bmatrix} \in \mathbf{R}^{250\times 250}, \tag{5.1}$$

having seven ones in the first row. This matrix can be set up in MATLAB with the command `A=gallery('grcar',250,6)`. From an inspection of $\Lambda(A)$ it is obvious that $\lambda_m = -1$ and that ϕ can be chosen slightly smaller than π. For simplicity we choose $\phi = 9\pi/10$. Because $\Lambda(A)$ is located roughly on a circle with radius $s = \max\ |Im(\Lambda(A))| \approx 2.0229$ around the origin, Ω_ϵ was scaled by s. Figure 4 shows the inclusion of $\Lambda(A)$ by $s\Omega_\epsilon$ for $\epsilon = 0.1$ and $\epsilon = 0.05$ ('$*$' indicates the origin). We point out that the sets $s\Omega_\epsilon$ for this example are comparable to pseudospectra of A (cf. [22, Figure 3.1]). Hence, a hybrid PIM using normalized Faber polynomials

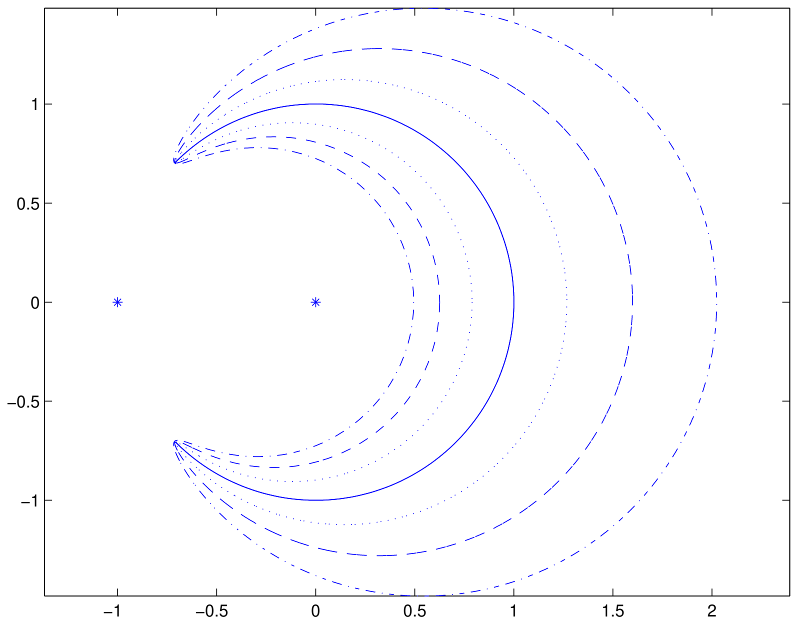

Figure 1: $\partial\Omega_\epsilon$ for $\Omega_\epsilon \in \mathbf{B}(-1, \pi/2)$, $\epsilon = 0$ (solid), 0.05 (dotted), 0.1 (dashed), 0.15 (dashdot)

for $s\Omega_\epsilon$ as residual polynomials will in this case feature polynomials that are small on pseudospectra of the coefficient matrix. According to observations of Nachtigal et al. [22, Section 2], this should lead to good performance.

The second example is the matrix $B = PDE225 \in \mathbf{R}^{225\times 225}$, which we downloaded from the `MatrixMarket` web site at URL

$$\texttt{http : //math.nist.gov/MatrixMarket}.$$

B is derived from a partial differential equation test problem. $\Lambda(B)$ is, for example, contained in the set $2\Omega_{1.18}$, where $\Omega_{1.18} \in \mathbf{B}(-1, 7\pi/6)$. Figure 5 shows the resulting plots ('$*$' indicates the origin).

The transfinite diameters and asymptotic convergence factors are listed below.

	A, $\epsilon = 0.1$	A, $\epsilon = 0.05$	B
$t(s\Omega_\epsilon)$	1.7937	1.6611	5.1911
$R(s\Omega_\epsilon)$	0.8068	0.7843	0.9563

Note that it would be difficult to include $\Lambda(A)$ or $\Lambda(B)$ in a set bounded by a circle or an ellipse not containing the origin.

Example 5.4 We study the zeros of Faber polynomials for elements of $\mathbf{B}(\lambda_m, \phi)$. As noted in Section 4, the zeros are identical to the eigenvalues of the matrix H_n in (4.15). Hence, the zeros can be computed by applying MATALB's `eig` function to H_n. In Figures 6 and 7 we plot the zeros of the Faber polynomial $F_{100}(z)$ for the sets $\Omega_{0.1} \in \mathbf{B}(-1, 9\pi/10)$ and $\Omega_{1.18} \in \mathbf{B}(-1, 7\pi/6)$, respectively. Note that the zeros are in both cases located in the interior and close to the boundary of the inclusion sets. Our numerical experience with these and further examples suggests that these distributions of zeros are typical for the Faber polynomials for elements of $\mathbf{B}(\lambda_m, \phi)$.

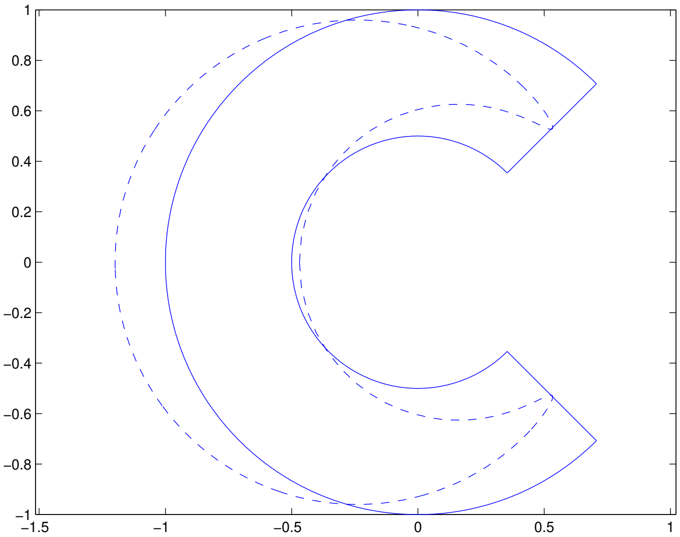

Figure 2: $\partial\mathbf{S}(1,\pi/2,1/2)$ (solid) and $\partial(\frac{3}{4}\Omega_{0.1})$ for $\Omega_{0.1} \in \mathbf{B}(1,\pi/2)$ (dashed)

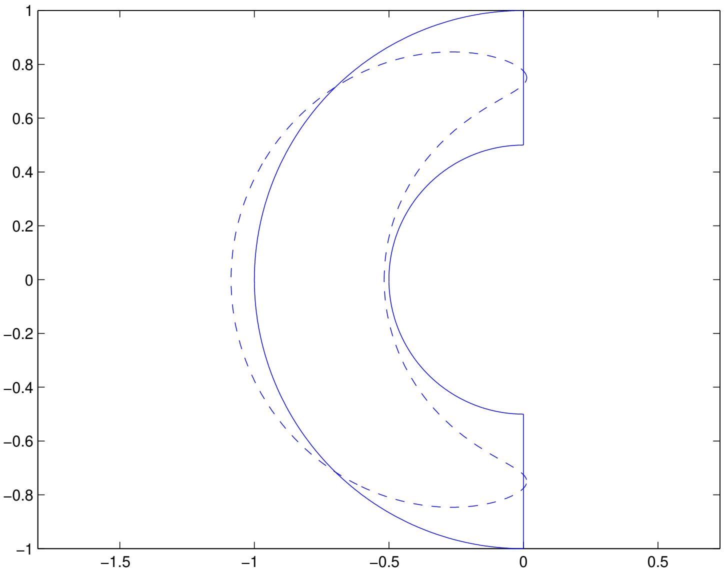

Figure 3: $\partial\mathbf{S}(1,\pi,1/2)$ (solid) and $\partial(\frac{3}{4}\Omega_{0.2})$ for $\Omega_{0.2} \in \mathbf{B}(1,\pi)$ (dashed)

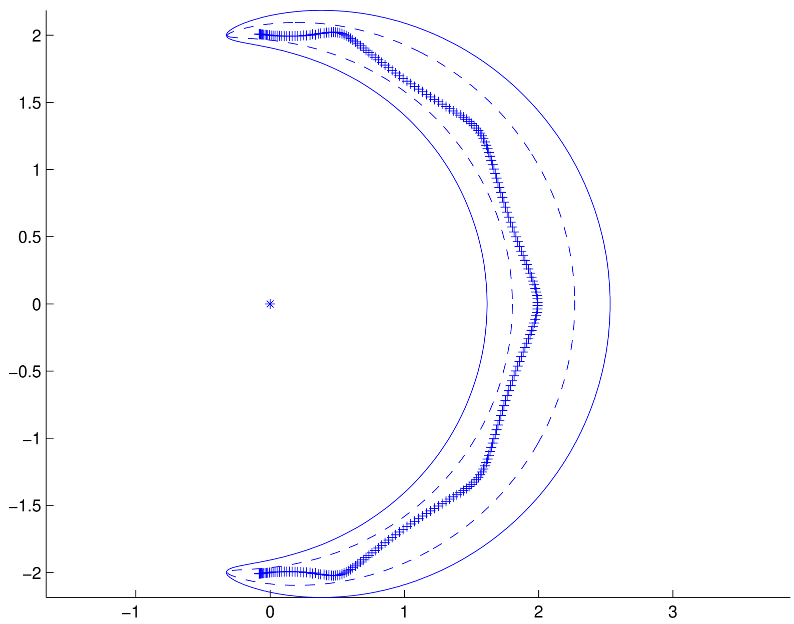

Figure 4: $\Lambda(A)$ (pluses) and $\partial(s\Omega_\epsilon)$ for $\Omega_\epsilon \in \mathbf{B}(-1, 9\pi/10)$, $s = \max\,|Im(\Lambda(A))|$, $\epsilon = 0.1$ (solid) and $\epsilon = 0.05$ (dashed)

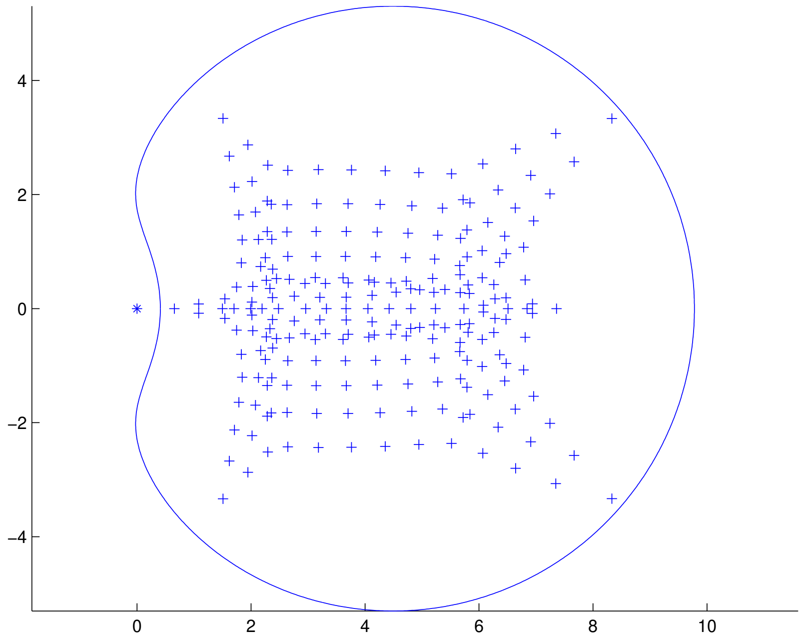

Figure 5: $\Lambda(B)$ (pluses) and $\partial(2\Omega_{1.18})$ for $\Omega_{1.18} \in \mathbf{B}(-1, 7\pi/6)$ (dashed)

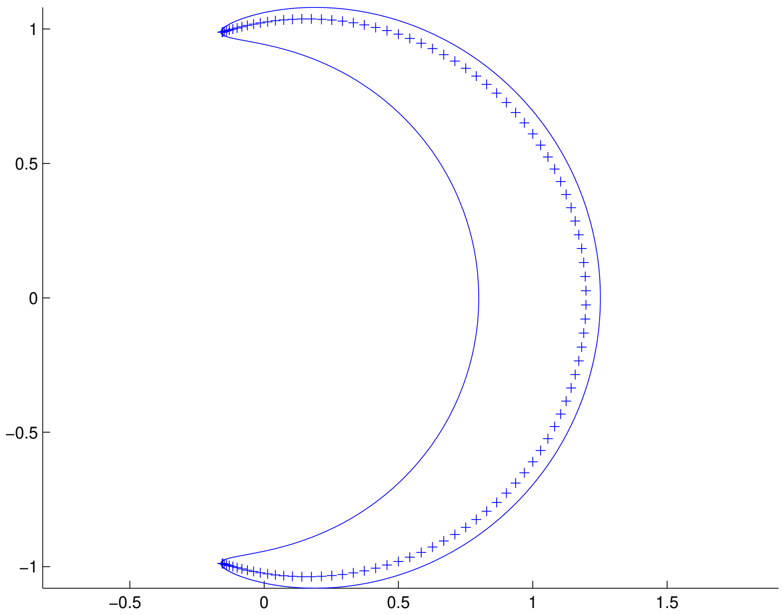

Figure 6: $\partial\Omega_{0.1}$ for $\Omega_{0.1} \in \mathbf{B}(-1, 9\pi/10)$ (solid) and the zeros of the corresponding Faber polynomial $F_{100}(z)$ (pluses)

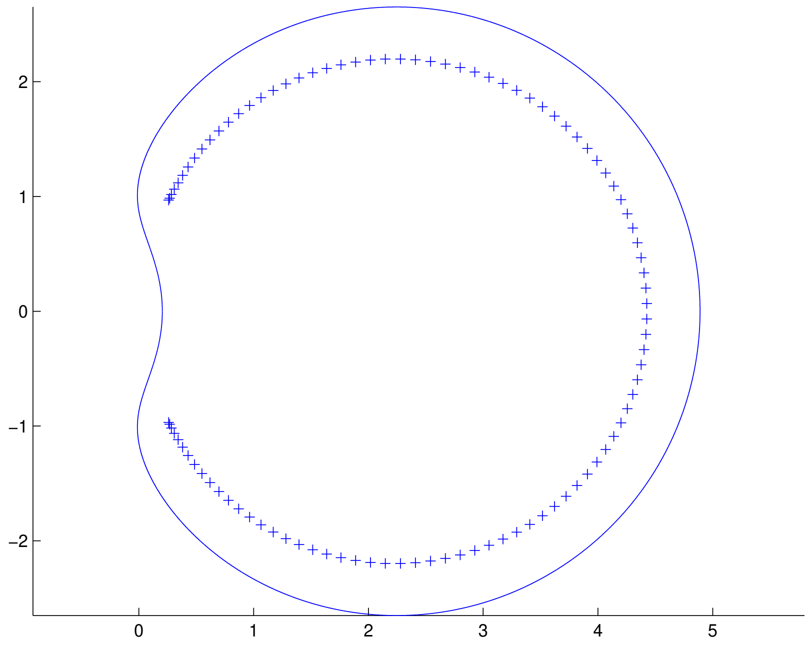

Figure 7: $\partial\Omega_{1.18}$ for $\Omega_{1.18} \in \mathbf{B}(-1, 7\pi/6)$ (solid) and the zeros of the corresponding Faber polynomial $F_{100}(z)$ (pluses)

As shown by Köravi and Pommerenke [17], the zeros of Faber polynomials for a convex set, which is not a line segment, are located in that set. It was later conjectured that the zeros of Faber polynomials for any set are always in the convex hull of the set. This conjecture is shown false in an example by Goodman [13], who considers Faber polynomials for certain circular arcs. In our notation, Goodman shows that when $\phi > 4 \arccos 3^{-1/2} \approx 3.8213$, then two of the three zeros of $F_3(z)$ for $\Omega_0 \in \mathbf{B}(-1, \phi)$ are outside the convex hull of Ω_0. We computed a numerical example: If $\phi = 3\pi/2$, then the absolute values of the zeros of $F_3(z)$ are approximately 0.9928 and 1.0020 (twice).

Note that Goodman considers sets without interior. However, using Goodman's result and the elements of $\mathbf{B}(\lambda_m, \phi)$, we can now easily construct sets with nonempty interior, for which the zeros of corresponding Faber polynomials are also outside the convex hull of the sets. We use the fact that the eigenvalues of the matrix H_n in (4.15) depend continuously on the parameters λ_m, ϕ and ϵ. If some $\phi_1 > 4 \arccos 3^{-1/2}$ is given, then the Faber polynomial $F_3(z)$ for $\Omega_0 \in \mathbf{B}(-1, \phi_1)$ has two zeros outside the convex hull of Ω_0. Because of the continuity, there exists some $\epsilon_1 > 0$, so that for each $\epsilon \in [0, \epsilon_1)$, the zeros of the Faber polynomial $F_3(z)$ for each $\Omega_\epsilon \in \mathbf{B}(\lambda_m, \phi_1)$ are outside the convex hull of Ω_ϵ as well. An example we computed numerically is given by the set $\Omega_{0.001} \in \mathbf{B}(-1, 3\pi/2)$, for which the zeros of $F_3(z)$ have absolute values of approximately 0.9931 and 1.0021 (twice), while the largest element in $\Omega_{0.001}$ has an absolute value of approximately 1.0008.

6 Acknowledgments

The first author is supported by the SFB 343 at the University of Bielefeld. The second author is supported by a Ph.D. grant of the Studienstiftung des deutschen Volkes. We thank Professor Ludwig Elsner for helpful discussions and careful reading of the manuscript. Further thanks go to Professor Zdeněk Strakoš for helpful discussions and for pointing out reference [20].

References

[1] J. P. Coleman and N. J. Myers. The Faber polynomials for annular sectors. *Math. of Comput.*, 64:181–203, 1995.

[2] J. Curtiss. Faber polynomials and the Faber series. *American Math. Monthly*, 78:577–596, 1971.

[3] M. Eiermann. On semiiterative methods generated by Faber polynomials. *Numer. Math.*, 56:139–156, 1989.

[4] M. Eiermann. Field of values and iterative methods. *In preparation*, 1996.

[5] H. C. Elman, Y. Saad, and P. E. Saylor. The hybrid Chebyshev Krylov subspace algorithm for solving nonsymmetric systems of linear equation. *SIAM J. Sci. Stat. Comput.*, 7:840–855, 1986.

[6] B. Fischer. Chebyshev polynomials for disjoint compact sets. *Const. Approx.*, 8:309–329, 1992.

[7] B. Fischer and R. Freund. On the constrained Chebyshev approximation on ellipses. *J. Approx. Theory*, 62:297–315, 1990.

[8] B. Fischer and R. Freund. Chebyshev polynomials are not always optimal. *J. Approx. Theory*, 65:261–272, 1991.

[9] R. Freund and S. Ruscheweyh. On a class of Chebyshev approximation problems which arise in connection with a conjugate gradient type method. *Numer. Math.*, 48:525–542, 1986.

[10] R. W. Freund, G. H. Golub, and N. M. Nachtigal. Iterative solution of linear systems. *Acta Numerica*, 1:57–100, 1992.

[11] R. W. Freund and N. M. Nachtigal. QMR: A quasi-minimal residual method for non-hermitian linear systems. *Numer. Math.*, 60:315–339, 1991.

[12] D. Gaier. *Vorlesungen über Approximation im Komplexen*. Birkhäuser Verlag, Basel, 1980.

[13] A. W. Goodman. A note on the zeros of Faber polynomials. *Proc. Amer. Math. Soc.*, 49:407–410, 1975.

[14] M. He. Numerical results on the zeros of Faber polynomials for m-fold symmetric domains. In *Exploiting symmetry in applied and numerical analysis (Fort Collins, CO, 1992)*, volume 29 of *Lectures in Appl. Math.*, pages 229–240. Amer. Math. Soc., Providence, RI, 1993.

[15] P. Henrici. *Applied and computational complex analysis.* Wiley, New York, 1986.

[16] E. Hille. *Analytic function theory. Vol. II.* Ginn and Co., Boston, Mass.-New York-Toronto, Ont., 1962.

[17] T. Kövari and C. Pommerenke. On Faber polynomials and Faber expansions. *Math. Z.*, 99:193–206, 1967.

[18] T. A. Manteuffel and G. Starke. On hybrid iterative methods for nonsymmetric systems of linear equations. *Numer. Math.*, 73(4):489–506, 1996.

[19] A. I. Markushevich. *Theory of functions of a complex variable. Vol. I.* Prentice-Hall Inc., Englewood Cliffs, N.J., 1965.

[20] J. Modersitzki and G. Opfer. Faber versus minimal polynomials on annular sectors. Preprint Reihe A 88, Hamburger Beitr. zur Angew. Math., 1994.

[21] N. M. Nachtigal, S. Reddy, and L. N. Trefethen. How fast are nonsymmetric matrix iterations? *SIAM J. Matrix Anal. Appl.*, 13:778–795, 1992.

[22] N. M. Nachtigal, L. Reichel, and L. N. Trefethen. A hybrid GMRES algorithm for nonsymmetric linear systems. *SIAM J. Matrix Anal. Appl.*, 13(3):796–825, 1992.

[23] V. Paatero. Über die konforme Abbildung von Gebieten deren Ränder von beschränkter Drehung sind. *Ann. Acad. Sci. Fenn. Ser. A.*, 33(9):1–77, 1931.

[24] C. Paige and M. Saunders. Solution of sparse indefinite systems of linear equations. *SIAM J. Numer. Anal.*, 12:617–629, 1975.

[25] Y. Saad and M. H. Schultz. GMRES: A generalized minimal residual algorithm for solving nonsymmetric linear systems. *SIAM J. Sci. Stat. Comput.*, 7:856–869, 1986.

[26] V. Smirnov and N. Lebedev. *Functions of a complex variable - Constructive theory.* The M.I.T. Press, Cambridge, MA, 1968.

[27] G. Starke and R. S. Varga. A hybrid Arnoldi-Faber method for nonsymmetric systems of linear equations. *Numer. Math.*, 64:213–240, 1993.

[28] The MathWorks. *Using MATLAB (December 1996).* The MathWorks Inc., Natick, 1996.

[29] J. Walsh. *Interpolation and approximation by rational functions in the complex domain.* American Mathematical Society, Providence, RI, 5th edition, 1969.

[30] A. Wathen, B. Fischer, and D. Silvester. The convergence rate of the minimal residual method for the Stokes problem. *Numer. Math.*, 71:121–134, 1995.